Simvastatin inhibits L-type Ca^{2+}-channel activity through impairment of mitochondrial function

Liam Curry*, Hani Almukhtar&, Jala Alahmed†, Richard Roberts‡ and Paul A. Smith§

School of Life Sciences

University of Nottingham

Nottingham

NG7 2UH

UK

*Email: liam.curry@ exmail.nottingham.ac.uk

&Email: hanialmukhtar@uomosul.edu.iq

† Email: mbxja1@exmail.nottingham.ac.uk

‡ Email: mbzrr@exmail.nottingham.ac.uk

§Corresponding author

Email: Paul.a.smith@nottingham.ac.uk

Tel: 44 115 849 3227

Fax: 44 115 823 0142

Abstract

Plasma membrane ion channels and mitochondrial electron transport complexes (mETC) are recognised "off-targets" for certain drugs. Simvastatin is one such drug, a lipophilic statin used to treat hypercholesterolaemia, but which is also associated with adverse effects like myopathy and increased risk of glucose intolerance. Such myopathy is thought to arise through adverse actions of simvastatin on skeletal muscle mETC and mitochondrial respiration. In this study we investigated whether the glucose intolerance associated with simvastatin is also mediated via adverse effects on mETC in pancreatic beta-cells since mitochondrial respiration underlies insulin secretion from these cells, an effect in part mediated by promotion of Ca^{2+} influx via opening of voltage-gated Ca^{2+} channels (VGCCs). We used murine pancreatic beta-cells to investigate these ideas. Mitochondrial membrane potential, oxygen consumption and ATP-sensitive-K^+-channel activity were monitored as markers of mETC activity, respiration and cellular ATP/ADP ratio respectively; Ca^{2+} channel activity and Ca^{2+} influx were also measured. In intact beta-cells, simvastatin inhibited oxidative respiration ($IC_{50} \sim 3$ μM) and mETC ($1 < IC_{50} < 10$ μM), effects expected to impair VGCC opening. Consistent with this idea simvastatin > 0.1 μM reversed activation of VGCCs by glucose but had no significant effect in the sugar's absence. The VGCC effects were mimicked by rotenone which also decreased respiration and ATP/ADP. This study demonstrates modulation of beta-cell VGCC activity by mitochondrial respiration and their sensitivity to mETC inhibitors. This reveals a novel outcome for the action of drugs like simvastatin for which mETC is an "off target".

Introduction

Mitochondrial electron transport (mETC) complexes (Nadanaciva *et al.*, 2007; Hargreaves *et al.*, 2016; Wallace, 2008) and plasma membrane ion channels are well recognised "off targets" for drugs (Lynch *et al.*, 2017; Real *et al.*, 2018). For some drugs, both moieties may be "off targets"; a situation which confounds the interpretation of adverse drug effects both in the clinic and laboratory. An example of this occurs in insulin secreting beta cells with the 3-hydroxy-3-methyl glutaryl coenzyme A (HMG-CoA) reductase inhibitor, simvastatin, a lipophilic drug used to treat hypercholesteremia. Such pluripotent effects of simvastatin complicates the mechanistic understanding of how adverse effects arise in the clinic; for example the association between lipophilic statin use and increased risk of glucose intolerance and diabetes (Cederberg *et al.*, 2015; Sattar *et al.*, 2010).

Insulin secretion from the pancreatic beta-cell is promoted by glucose via oxidative metabolism (Maechler *et al.*, 2010; Affourtit *et al.*, 2018). The resultant increase in cytosolic ATP/ADP ratio blocks the activity of ATP-sensitive K^+ channels (K_{ATP}) which leads to depolarization of the plasma-membrane potential (Vm) and activation of voltage-gated Ca^{2+} channels (VGCCs). Ca^{2+} influx through VGCCs promotes insulin secretion (Ashcroft *et al.*, 1994). In pancreatic β-cells mitochondrial respiration is shown to enhance L-type VGCC activity (Smith *et al.*, 1989).

Several "off targets" for simvastatin are recognised in β-cells. For example chronic simvastatin impairs mitochondrial respiration and ATP production (Zhou *et al.*, 2014; Urbano *et al.*, 2017). Such chronic effects are mediated by a decrease in activity of the mETC complexes (Urbano *et al.*, 2017) with an associated impairment in ATP production (Zhou *et al.*, 2014; Urbano *et al.*, 2017). Simvastatin likewise disrupts mETC ($IC_{50} \sim 2$ μM) in skeletal muscle to depolarize the inner mitochondrial membrane potential ($\Delta\Psi_{mit}$; Sirvent, Mercier, *et al.*, 2005). Consequently an impairment in mitochondrial function is expected to decrease VGCC activity and Ca^{2+} influx, events that will suppress insulin secretion. Indeed a similar

mechanism has already been proposed to explain the decrease in artery vascular smooth muscle tone seen with statins (Almukhtar *et al.*, 2016); a tissue in which VGCCs are also modulated by ATP and mitochondrial respiration (McHugh and Beech, 1996; Ohya and Sperelakis, 1989).

The aims of the present study were to investigate these ideas and determine if simvastatin can adversely affect the activity of L-type Ca^{2+} channels in pancreatic β-cell indirectly via mitochondrial effects and in doing so reveal a novel outcome for the action of drugs for which mETC is an "off target".

Materials and methods

Preparation of β-cells

For this study murine beta-cells were used (Daunt *et al.*, 2006). Primary pancreatic beta-cells were dissociated from islets of male CD1 mice (30-35 g) as described (Smith *et al.*, 1999). Mice were stunned by cervical dislocation and killed by decapitation. Islets were extracted by collagenase digestion and single cells liberated by dissociation with trypsin-EDTA. Cells were maintained in RPMI 1640 media, supplemented with 11 mM glucose, 10 % FBS, 10 mM HEPES, 50 µg/ml penicillin and streptomycin. Cells were kept up to 2 days in a humidified atmosphere of 5% CO_2/95% at 37 °C. All animal care and experimental procedures were carried out in accordance with the UK Home Office Animals (Scientific Procedures) Act (1986). To reduce and replace animal use, the murine beta-cell line MIN6 (Daunt *et al.*, 2006; Smith *et al.*, 2001) were used for measurement of K_{ATP} and L-type Ca^{2+} channel activity, Ca^{2+} imaging and beta-cell respiration. MIN6 cells, passage 35-40 were from our own stock and were sourced as originally described (Smith *et al.*, 2001); these were maintained as for primary beta-cells but without antibiotics. The suitability of MIN6 cells as a model system in which to study mitochondrial function of beta-cells has already been argued (Elmorsy *et al.*, 2017).

Mitochondrial respiration

The rate of oxygen consumption (OCR) was used to measure mitochondrial respiration *in-situ* with Clark oxygen electrodes (Rank Brothers, Bottisham, UK) as previously described (Daunt *et al.*, 2006). Known densities of MIN6 cells were incubated at 32^oC in Hanks solution which contained (in mM): 137 NaCl, 5.6 KCl, 1.2 $MgCl_2$, 2.6 $CaCl_2$, 1.2 NaH_2PO_4, 4.2 $NaHCO_3$ 10 HEPES (pH 7.4 with NaOH). For OCR cells were first incubated in the absence of substrate, basal, followed by stimulation with10 mM glucose for 10 minutes after which a single concentration of drug was tested. The OCR was corrected for background consumption of O_2 by the electrode by subtraction of the OCR measured in 6 mM NaN_3, a treatment which blocks oxidative respiration at mETC complex IV. The effect of drugs is expressed as the change in OCR relative to that stimulated by glucose in the same suspension. Only data from glucose-sensitive suspensions was used (>10% increase in response to 10 mM glucose).

Imaging studies

Changes in inner mitochondrial membrane potential ($\Delta\Psi_{mit}$) and cytosolic calcium concentration ($[Ca^{2+}]_i$) were monitored with rhodamine-123 (Rh123) and the calcium fluophore FLUO-4 respectively as previously described (Daunt *et al.*, 2006; Duchen *et al.*, 1993). Cells were perifused in a modified Hanks solution at 32^oC. Regions of interest (ROI) were drawn around cells, corrected for background fluorescence by subtraction, and the average fluorescence intensity calculated. To sample the total cell population, ROIs were from both single cells and cell clusters. For each experimental group, samples were pooled from multiple visual fields from at least 4 different cell preparations. Image analysis was performed with custom scripts written in Labtalk (OriginLab Corporation, MA USA).

For $\Delta\Psi_{mit}$, images were captured at a frame rate of 1 Hz with a Photonics ISIS CCD camera, DT3155 frame grabber (Data Translation, UK) and Imaging workbench software (IW6 INDEC BioSystems, Santa Clara, USA). Only ROIs that responded 1 µM FCCP (carbonyl

cyanide-4-(trifluoromethoxy) phenylhydrazone), a mitochondrial protonophore which collapses $\Delta\Psi_{mit}$ and results in a fluorescence increase, were chosen for further analysis (Duchen *et al.*, 1993; Elmorsy *et al.*, 2017). ROIs were normalised to the difference between the fluorescence measured in glucose (minimum fluorescence) and that in and that in the presence of 1 µM FCCP (maximum fluorescence) (Daunt *et al.*, 2006).

For $[Ca^{2+}]_i$ images were captured at 1 Hz with a Coosnap HQ2 camera (Photometrics, UK) and Imaging workbench software. Only cells that responded to 10 mM glucose with an increase in steady-state $[Ca^{2+}]_i$ greater than 10% compared to basal were chosen for further analysis. To calibrate $[Ca^{2+}]_i$, fluorescence changes were calibrated by a one-point method that involved permeabilization of the cells with saponin (0.01-0.1 % wt/v), with the maximum fluorescence value observed taken as Fmax. To calculate $[Ca^{2+}]_i$ the following equation was used (Equation 1):

$$[Ca^{2+}]_i = Kd \times \frac{F}{Fmax - F}$$

Where F is the fluorescence (background subtracted), and Kd is the dissociation constant of Fluo-4: 345 nM. To quantify changes in $[Ca^{2+}]_i$, its mean (µ) and standard deviation (σ) were calculated for the last 60 seconds of any given treatment, a period over which $[Ca^{2+}]_i$ sustained a steady state. The variation in $[Ca^{2+}]_i$, as indicated by $\sigma[Ca^{2+}]_i$, was assumed to be indicative of underlying calcium-dependent action potential activity (Rorsman *et al.*, 1992). For statistical analysis $\mu[Ca^{2+}]_i$ and $\sigma[Ca^{2+}]_i$ were normalised as percentage of that measured for glucose alone in the same ROI: $\Delta\mu[Ca^{2+}]_i$ and $\Delta\sigma[Ca^{2+}]_i$ respectively.

Measurement of L-type Ca^{2+} channel activity

Measurement of L-type Ca^{2+} activity was performed with cell-attached patch-clamp, similar to that described (Smith *et al.*, 1989). This method was used preferentially over whole-cell methods (Smith *et al.*, 1989; Smith, 2009) to prevent K^+ channel contamination.

Patch pipettes were drawn from GC150TF capillary glass (Harvard Instruments), coated with Sylgard (Dow-Corning) and fire polished before use. Pipettes typically had resistances between 2-4 MΩ. The zero-current potential was adjusted with the pipette in the bath just before seal establishment. No corrections have been made for liquid junction potentials (<4 mV). Currents were low pass filtered at 2 kHz (–3db, 8 pole Bessel), digitized at 10 kHz using pClamp 8.3 (Axon Instruments, Foster City, USA).

To maximize channel detection, but minimize surface charge effects (Smith *et al.*, 1993) the pipette contained (in mM): 0.1 μM BAY-K8644, 140 NaCl, $BaCl_2$ 10, HEPES 10 (pH 7.4 with NaOH). Cells were bathed in a high K^+ Hanks solution which contained (in mM): 140 KCl, 3.8 $MgCl_2$, 1.2 NaH_2PO_4, 4.2 $NaHCO_3$ 10 HEPES (pH 7.4 with NaOH); a solution which electrochemically clamps Vm to 0mV.

To record single Ca^{2+} channel activity, Vm was held at -90 mV and Ca^{2+} currents were elicited by pulses to -40 mV of 200 ms duration at 0.5 Hz. Leak and capacitance currents were removed by subtraction of the numerical average of records absent of activity. Channel activity, NPo, was recorded for 3-5 minutes, first in basal then after 10 minute incubation in 10 mM glucose, followed by the addition of drug or vehicle.

Single-channel data were analysed with custom scripts written in Labtalk using half-amplitude threshold techniques as described (Smith *et al.*, 1993). Drug effects on NPo were quantified as a percentage of its respective control values. Ca^{2+} currents are displayed conventionally as downward deflections.

Assessment of intracellular ATP: Cell-attached K_{ATP} ion channel activity as a biosensor

To monitor the acute intracellular ATP/ADP ratio, the activity of K_{ATP} channels in cell-attached experiments was measured. This channel acts as a biosensor of the intracellular sub membrane ATP/ADP ratio and can be used to follow the energetic status of an intact cell in real time (Gribble et al., 2000). For this, K_{ATP} channel activity was measured in cell-attached experiments with a pipette potential, Vp, of 0 mV. The pipette contained (in mmol/l):

140 KCl, CaCl2 2.6, MgCl$_2$ 1.2, HEPES 10 (pH 7.4 with NaOH). K$_{ATP}$ currents were low pass filtered at 2 kHz (–3db, 8 pole Bessel) and digitized at 10 kHz using PClamp. Single-channel data were analysed with half-amplitude threshold techniques as implemented in Clampfit Ver. 10.6 (Axon Instruments, Foster City, USA). Channel activity, NPo, was measured continuously, in the absence then presence of 10 mM glucose followed by drug additions. An increase in NPo reflects a decrease in ATP/ADP (Gribble et al., 2000); a phenomenon expected to occur with an impairment of glucose metabolism (Köhler et al., 1998; Kiranadi et al., 1991).

Drugs

Simvastatin and pravastatin were obtained from Tocris Bioscience, Bristol, UK. FCCP was obtained from Sigma-Aldrich, Poole, UK. Simvastatin was used in its lipophilic, lactone, form. Simvastatin, rotenone and FCCP were dissolved in ethanol or DMSO; Pravastatin was dissolved in H$_2$O. Drug additions were made from serially diluted stocks such that the vehicle was always applied at the same final concentration; for the electrophysiology this was 0.1% vol/vol and for the OCR this was 1% vol/vol.

Statistical Analysis

Statistical analysis was performed using either Graphpad PRISM version 7.03 (San Diego, California USA) or StatsDirect 3.1 (Cambridge, UK), data were tested with the D'Agostino & Pearson omnibus normality test and the appropriate statistical test used as given in the text. The concentration-response relationship for the block of OCR by simvastatin was quantified by fitting the data with the equation:

$$Y = 1/(1 + ([S] / IC_{50})^h)$$

Where Y is the fractional OCR, relative to that measured under control conditions, h is the slope index, [S] is the free simvastatin concentration and IC$_{50}$ the concentration that produces half-maximal inhibition. Since 0.1% BSA binds simvastatin to decrease its free

concentration ~10 fold (Shi *et al.*, 2017; Real *et al.*, 2018), [S] was taken to be 1/10th of the added concentration.

Data are quoted as either the mean ± SEM or median with 5 to 95% confidence intervals (C.I.), where n is the number of separate determinations. Statistical significance is defined as P <0.05 and is flagged in graphics as *, ** (p<0.01) or *** (p<0.001).

Results

Simvastatin blocks oxidative respiration.

In 5 mM glucose the $Δψ_{mit}$ of primary mouse beta-cells was hyperpolarised, as revealed by a reversible increase in Rh123 fluorescence on removal of the sugar (Figs. 1A, 1E). Addition of 1 µM FCCP dissipated $Δψ_{mit}$ and maximized Rh123 fluorescence (Duchen *et al.*, 1993). The effects of glucose and FCCP on $Δψ_{mit}$ were similar to those previously described in both MIN6 and primary beta-cells (Duchen *et al.*, 1993; Daunt *et al.*, 2006; Elmorsy *et al.*, 2017; Smith *et al.*, 1999). In the presence of glucose, 10 µM simvastatin depolarised $Δψ_{mit}$ (Fig. 1B). This effect consisted of an initial transient increase in Rh123 fluorescence superimposed upon an upward trend sometimes with stepwise increases. In Fig 1B, 10 µM simvastatin only partially collapsed $Δψ_{mit}$, since $Δψ_{mit}$ was dissipated on addition of 1 µM FCCP. Overall, 10 µM simvastatin depolarised $Δψ_{mit}$ by ~90% relative to its DMSO vehicle control (Fig. 2A; Kruskal Wallis, Dunn's multiple comparison test); neither 10 µM of the hydrophilic statin pravastatin (Figs. 1C, 2A) nor its solvent (0.1% vol/vol DMSO) affected $Δψ_{mit}$ (Fig. 2A). At 3 µM, simvastatin produced variable but significant decreases in $Δψ_{mit}$, smaller in magnitude than that seen with 10 µM of the drug (Fig. 2A). Simvastatin at 1 µM failed to affect $Δψ_{mit}$, even after 75 minutes incubation, the longest period tested (Figs. 1D, 2A). These data suggest that the IC_{50} for $Δψ_{mit}$ depolarization by simvastatin lies between 1 to 10 µM. At 1 µM, rotenone the positive control, depolarized $Δψ_{mit}$ (Fig 1E) like that seen with 3-10 µM simvastatin (Fig 2A; Kruskal Wallis, Dunn's multiple comparison test).

To further investigate the concentration effect of simvastatin on mitochondrial function, oxidative respiration, a direct measure of metabolic flux, was measured in the murine beta-cell line MIN6 (Daunt *et al.*, 2006). Glucose increased oxygen consumption rate (OCR) by 200 ± 24 % (n = 51) a value similar to that previously reported for this cell line (Elmorsy *et al.*, 2017; Daunt *et al.*, 2006). At a clinically relevant concentration of 10 nM (Björkhem-Bergman *et al.*, 2011), simvastatin did not affect OCR. However, at higher concentrations simvastatin blocked OCR with an IC_{50} of 3.1 µM (2.1 to 4.6 µM, 95% C.I.) and slope coefficient of -0.8 (-0.6 to -1.0, 95% C.I.; Fig 2B). At 1 µM, rotenone blocked OCR by ~70%, an amount greater than that of the highest concentration of simvastatin tested. (Fig 2B).

Simvastatin inhibits glucose stimulated Ca^{2+} influx

To determine if the inhibitory effect of simvastatin on mitochondrial respiration was manifest on Ca^{2+} influx, cytosolic Ca^{2+} was measured in MIN6 beta-cells. In the absence of glucose, basal $[Ca^{2+}]_i$ was 78 nM (, 63 to 107, 95% C.I.; Fig 3A). After a delay of between 1 to 4 minutes, 10 mM glucose produced an initial decrease in $[Ca^{2+}]_i$ followed by a biphasic increase. The latter consisted of an initial peak in $[Ca^{2+}]_i$ which then decayed to an elevated level of 120 nM (100 to 156, 95% C.I.; Fig 3A); a value 1.5 fold (1.4 to 1.7, 95% C.I.) greater than basal ($p < 0.0001$, Wilcoxon signed rank test). The latter was associated with transitory spikes indicative of underlying Ca^{2+}-dependent action potential activity (Rorsman *et al.*, 1992). In the presence of the sugar, 10 µM but not 1 µM simvastatin caused a significant decrease in both the average $[Ca^{2+}]_i$ (Fig. 3B; $p < 0.05$, Students t-test) and its associated variance or spiking activity (Fig. 3C; $p < 0.01$, Mann-Whitney test) relative to the DMSO vehicle control.

Simvastatin reverses glucose-stimulation of L-type Ca^{2+} channel activity

Since L-type Ca^{2+} channels in this cell type are regulated by mitochondrial respiration (Smith *et al.*, 1989), and simvastatin inhibited mETC and oxidative respiration, the action of the drug on VGCCs in functionally intact cells was explicitly explored with the cell-attached patch-clamp technique (Smith *et al.*, 1989). Figure 4 shows that membrane potential depolarization elicited single-channel activity in MIN6 beta-cells indicative of L-type voltage-gated Ca^{2+} channels that are found in pancreatic beta-cells (Smith *et al.*, 1993; Schulla *et al.*, 2003): voltage-dependent activation, a single channel current amplitude of ~ 1 pA at -40 mV and prolongation of open channel lifetimes by 0.1 µM BAY-K8644, a dihydropyridine L-type Ca^{2+} channel agonist (Smith *et al.*, 1989, 1993). Perifusion of glucose significantly increased channel activity (NPo) to 210 ± 9 % of basal (p = 0.013, Wilcoxon signed rank test relative to control, n = 14; Figs. 4B & D); an increase similar in magnitude to that previously reported for this channel in primary beta-cells (Smith *et al.*, 1989). Figure 4C shows that subsequent addition of 1 µM simvastatin reversed the effect of glucose and decreased NPo back down to its basal value (Fig 4D; p <0.0001, Kruskal Wallis Dunn's multiple comparison test). In the absence of glucose 1 µM simvastatin failed to affect channel activity (Fig. 4D; One sample t-test). Similar results were also seen with 10 µM simvastatin: a reversal of the stimulatory effect of 10 mM glucose on channel activity but with no effect in the absence of the sugar (Fig. 4D); these data are indicative of an indirect, glucose-dependent effect of simvastatin on this channel type. This latter idea is supported by the observation that the degree of inhibition in NPo produced by 1 µM simvastatin was linearly correlated (R^2 > 0.91; p<0.001, Pearson R) with the magnitude of increase in NPo stimulated by glucose (Fig. 4E). Figure 4D also shows that the ability of simvastatin to reverse the stimulatory effect of glucose on L-type Ca^{2+} channel activity was mimicked by 1 µM rotenone, an established inhibitor of mETC and mitochondrial respiration.

Rotenone but not Simvastatin reactivate glucose-blocked K_{ATP} channel activity

To investigate if $\Delta\psi_{mit}$ depolarization was associated with a decrease in intracellular ATP levels, the level of sub-membrane ATP was monitored indirectly by measurement of K_{ATP} channel activity in cell-attached patches (Gribble *et al.*, 2000; Köhler *et al.*, 1998; Kiranadi *et al.*, 1991). Figure 5 demonstrates the decrease in K_{ATP} channel activity associated with the rise in intracellular ATP/ADP that occurs with oxidative metabolism of glucose (Köhler *et al.*, 1998; Kiranadi *et al.*, 1991). Subsequent addition of 1 µM rotenone led to an increase in channel activity (Figs. 5F 5G), whereas 1 µM FCCP produced an even larger increase (Fig. 5g) to effectively reverse the inhibitory effect of glucose on K_{ATP} channel activity. Addition of 10 µM of simvastatin failed to mimic the ability of rotenone to reactivate K_{ATP} channels blocked by glucose, but instead produced further inhibition (Figs. 5c, 5G); an effect previously shown to be due to a direct block of the channel protein itself by this drug (Real *et al.*, 2018). Antimycin at 1 µM, similarly activated K_{ATP} like FCCP. Channel identity was confirmed by its abolition with 200 µM tolbutamide; a specific sulphonylurea inhibitor of K_{ATP} channels.

Discussion

In the pancreatic beta-cell, the lipophilic lactone form of the statin, simvastatin at concentrations greater than 1 µM depolarised $\Delta\psi_{mit}$, reversed the glucose activation of L-type Ca^{2+} channels and inhibited glucose-stimulated Ca^{2+} influx. In contrast, 10 µM of the hydrophilic statin pravastatin neither affected $\Delta\psi_{mit}$ or Ca^{2+} channel activity. Since all the effects of simvastatin were mimicked by rotenone, which also decreased the intracellular ATP/ADP ratio, supports the idea that this statin mediates its toxic effect on VGCCs via inhibition of oxidative respiration and a decrease in intracellular ATP/ADP; not by a direct action on the ion channel itself

Effect of simvastatin on mitochondrial membrane potential and respiration

We show that in pancreatic β-cells acutely applied simvastatin depolarizes $\Delta\psi_{mit}$. In most cells tested 10 µM, simvastatin collapsed $\Delta\psi_{mit}$, whereas at 3 µM it produced more variable affects, whilst at 1 µM it was without detectable effect. These results suggest that the IC_{50} for the lipophilic statin effect on mitochondrial function lies between 1 to 10 µM; a range that encompasses the IC_{50} of 3 µM for OCR; a potency similar to that seen in skeletal muscle: IC_{50} ~2 µM (Sirvent, Mercier, *et al.*, 2005). Although the IC_{50} value we report is extracellular in origin this is probably representative of the value experienced by the mETC since our MIN6 cell line do not possess p-glycoprotein that would affect cellular levels of lipophilic drugs (Daunt *et al.*, 2006), moreover simvastatin has been reported to block p-glycoprotein (Wang *et al.*, 2001). Based on data from respiration studies on intact mitochondria, it is argued that Complex I is the primary target for simvastatin (Sirvent, Bordenave, *et al.*, 2005); an idea support by the similarly of the effects of rotenone, a selective complex I inhibitor, to simvastatin in the present study. The inability of hydrophilic pravastatin to affect mitochondrial function is consistent with that previously reported for murine beta-cells (Zhou *et al.*, 2014) and porcine coronary artery (Almukhtar *et al.*, 2016).

The reason that the lipophilic statin simvastatin in its lactone form (logP 4.68) affects mitochondrial function, whereas a lipophobic statin such as pravastatin (logP 0.59) does not, probably relates to their ability to penetrate the inner mitochondrial membrane and gain access to either an intramembrane binding sites on the complexes (Degli Esposti, 1998) or disrupt membrane protein–lipid interactions (Hwang *et al.*, 2003). Indeed, the ability of certain drug classes to inhibit mETC in isolated mitochondria has already been related to their lipophilicity (logP values) (Durazo *et al.*, 2011). Similar ideas are also proposed to explain the ability of lipophilic compounds to directly block K_{ATP}-channels in the plasma membrane (Real *et al.*, 2018; Hwang *et al.*, 2003). The stepwise depolarizations in $\Delta\psi_{mit}$ that were occasionally observed with simvastatin may result from the random fusion of intracellular simvastatin aggregates; where lipophilic drugs can sometimes form intracellular

aggregates on penetration into the cell, such has been observed with clofazimnine (logP 7.5) (Baik and Rosania, 2011).

Effect of simvastatin on L-type Ca^{2+} channel activity.

L-type VGCCs are positively modulated by Mg^{2+} nucleotide complexes (O'Rourke *et al.*, 1992; Ohya and Sperelakis, 1989), such that changes in the cytosolic ATP/ADP ratio are expected to affect the activity of these ion channels. Indeed, both increases and decreases in the activity of L-type VGCCs in response to metabolic stimulation and mitochondrial inhibition respectively has already been described for both pancreatic beta-cells (Smith *et al.*, 1989) and smooth muscle (McHugh and Beech, 1996). Our observations that glucose stimulated L-type VGCCs activity and that both simvastatin and rotenone reversed this effect, are consistent with this idea, where a depolarization in $\Delta\psi_{mit}$, like that produced by simvastatin and rotenone, is known to decrease the cytosolic ATP/ADP ratio (Duchen *et al.*, 1993) and inhibit this channel. Indeed, we too demonstrate that rotenone can decrease the cytosolic ATP/ADP ratio as illustrated by its ability to activate K$_{ATP}$ channels blocked by glucose like that observed for other chemical disruptors of mitochondrial function such as antimycin, FCCP and others (Köhler *et al.*, 1998; Kiranadi *et al.*, 1991). We presume that simvastatin also decreases the cytosolic ATP/ADP given it ability to inhibit OCR and depolarize $\Delta\psi_{mit}$ just like rotenone. However these effects of simvastatin were not associated with activation of the K$_{ATP}$ channel since they were masked by the potent ability of simvastatin to directly interact with the ion channel protein and inhibit it as we have previously demonstrated (Real *et al.*, 2018).

Our data are consistent with whole-cell voltage-clamp studies on pancreatic beta-cells where simvastatin blocked L-type Ca^{2+} currents with an IC$_{50}$ of 2 µM (Yada *et al.*, 1999), a value similar to what we found for oxidative respiration. Although, other lipophilic compounds, such as Triton X-100 (Narang *et al.*, 2013) and barbiturates (Kozlowski and Ashford, 1991) can also block L-type Ca^{2+} channels they appear to do so via a direct,

anaesthetic-like, mechanism. The fact that the inhibition of VGCC activity was glucose-dependent and was mimicked by rotenone suggest that this block is mechanistically indirect and occurs via an inhibition of oxidative respiration and decreased metabolic regulation of this channel type. This idea is supported by the fact that simvastatin failed to affect the L-type Ca^{2+} channel in the absence of glucose and only abolished the stimulatory effect of glucose. Indeed, one technical advantage of the cell-attached patch clamp method over other configurations is that the cell is maintained in an intact functional state. This means that mitochondrial metabolism and signalling pathways continue to modulate channel activity within the patch.

We also demonstrate that the use of micromolar concentrations of simvastatin to study mitochondrial actions preclude any parallel investigation of changes in K_{ATP}-channel activity that may result from an alteration in cytosolic ATP due to the fact that this drug acts to directly block and silence this particular ion channel species as we reported previously (Real *et al.*, 2018).

Effect of simvastatin on Ca^{2+} influx.

The reduction in the $[Ca^{2+}]_i$ variance we observed with 10 µM simvastatin is consistent with a decline in the Ca^{2+} dependent electrical activity that would result from a decrease in L-type Ca^{2+} channel activity (Rorsman *et al.*, 1992). The observation that 1 µM simvastatin was effective in the patch-clamp studies but failed to affect intracellular Ca^{2+} levels may relate to the dissimilarity in temperatures employed: 22°C and 32°C respectively. Since oxidative respiration in these cells has a Q_{10} of 5 (Ohta *et al.*, 1990; Escolar *et al.*, 1990) a greater concentration of simvastatin may be required to block the higher metabolic flux of glucose-metabolism at 32°C. This reason may also contribute to the explanation of why, in a previous study (Real *et al.*, 2018), we failed to see an effect of 1 µM simvastatin on glucose stimulated insulin secretion at 32°C.

Physiological Implications

The concentrations of simvastatin that we found to acutely affect mitochondrial function and VGCC activity (1-10 μM) are similar to those used in other *in-vitro* studies (Ishikawa *et al.*, 2006; Zhou *et al.*, 2014; Sirvent, Mercier, *et al.*, 2005), but are in excess of those normally measured clinically (0.1-10 nM) (Björkhem-Bergman *et al.*, 2011). It should be noted that in many previous studies, the effects of simvastatin on pancreatic beta-cell function looked at long term effects after chronic incubation of many hour to days, whereas here we have investigated acute effects on the minute to minute time scale . Under certain circumstances, e.g. drug interactions, plasma levels of simvastatin can reach ~1 μM (Lilja *et al.*, 1998): a concentration sufficiently high enough to elicit mitochondrial dysfunction in pancreatic beta-cells and perhaps contribute to the diabetogenic effect of this particular class of drug. The ability of simvastatin to impair beta-cell function arises from at least two mechanisms: via a direct block of K_{ATP} channels at nanomolar concentrations which is mitochondrial independent. Whereas at higher, micromolar, concentrations mitochondria respiration is impaired to decrease cytosolic ATP levels and inhibit metabolic regulation of L-type Ca^{2+} channels. In fact, the actual impact on insulin secretion will be the result of a convolution of these two process combined with other ATP-dependent process that will also be compromised such as exocytosis (Eliasson *et al.*, 1996).

In conclusion our data highlights the fact that the cellular toxicity of an agent, which can acutely target and impair mitochondrial function, may in part result from decreased L-type Ca^{2+} channel activity, Ca^{2+} influx and compromised cell functions that are Ca^{2+} dependent.

Conflict of interest

No authors have a conflict of interest that might bias their work and have nothing to declare

References

Affourtit, C. *et al.* (2018) Control of pancreatic β -cell bioenergetics. *Biochem. Soc. Trans.*, **46**, 555–564.

Almukhtar, H. *et al.* (2016) Effect of simvastatin on vascular tone in porcine coronary artery: Potential role of the mitochondria. *Toxicol. Appl. Pharmacol.*, **305**, 176–185.

Ashcroft, F.M. *et al.* (1994) Stimulus-secretion coupling in pancreatic β cells. *J. Cell. Biochem.*, **55**, 54–65.

Baik, J. and Rosania, G.R. (2011) Molecular imaging of intracellular drug-membrane aggregate formation. *Mol. Pharm.*, **8**, 1742–1749.

Björkhem-Bergman, L. *et al.* (2011) What is a relevant statin concentration in cell experiments claiming pleiotropic effects? *Br. J. Clin. Pharmacol.*, **72**, 164–165.

Cederberg, H. *et al.* (2015) Increased risk of diabetes with statin treatment is associated with impaired insulin sensitivity and insulin secretion: a 6 year follow-up study of the METSIM cohort. *Diabetologia*, **58**, 1109–1117.

Daunt, M. *et al.* (2006) Somatostatin inhibits oxidative respiration in pancreatic β-cells. *Endocrinology*, **147**, 1527–1535.

Degli Esposti, M. (1998) Inhibitors of NADH-ubiquinone reductase: An overview. *Biochim. Biophys. Acta - Bioenerg.*, **1364**, 222–235.

Duchen, M.R. *et al.* (1993) Substrate-dependent changes in mitochondrial function, intracellular free calcium concentration and membrane channels in pancreatic β-cells. *Biochem. J.*, **294**, 35–42.

Durazo, S.A. *et al.* (2011) Brain mitochondrial drug delivery: Influence of drug physicochemical properties. *Pharm. Res.*, **28**, 2833–2847.

Eliasson, L. *et al.* (1996) Endocytosis of secretory granules in mouse pancreatic β-cells evoked by transient elevation of cytosolic calcium. *J. Physiol.*, **493**.

Elmorsy, E. *et al.* (2017) Therapeutic concentrations of antidepressants inhibit pancreatic
beta-cell function via mitochondrial complex inhibition. *Toxicol. Sci.*, **158**, 286–301.

Escolar, J.C. *et al.* (1990) Effect of low temperatures on glucose-induced insulin secretion
and glucose metabolism in isolated pancreatic islets of the rat. *J. Endocrinol.*, **125**,
45–51.

Gribble, F.M. *et al.* (2000) A novel method for measurement of submembrane ATP
concentration. *J. Biol. Chem.*, **275**, 30046–30049.

Hargreaves, I.P. *et al.* (2016) Drug-Induced Mitochondrial Toxicity. *Drug Saf.*, **39**, 661–
674.

Hwang, T.C. *et al.* (2003) Genistein Can Modulate Channel Function by a
Phosphorylation-Independent Mechanism: Importance of Hydrophobic Mismatch and
Bilayer Mechanics. *Biochemistry*, **42**, 13646–13658.

Ishikawa, M. *et al.* (2006) Distinct effects of pravastatin, atorvastatin, and simvastatin on
insulin secretion from a beta-cell line, MIN6 cells. *J. Atheroscler. Thromb.*, **13**, 329–
335.

Kiranadi, B. *et al.* (1991) Inhibition of electrical activity in mouse pancreatic β-cells by the
ATP/ADP translocase inhibitor, bongkrekic acid. *FEBS Lett.*, **283**, 93–96.

Köhler, M. *et al.* (1998) Changes in cytoplasmic ATP concentration parallels changes in
ATP-regulated K+-channel activity in insulin-secreting cells. *FEBS Lett.*, **441**, 97–102.

Kozlowski, R.Z. and Ashford, M.L.J. (1991) Barbiturates inhibit ATP-K+ channels and
voltage-activated currents in CRI-G1 insulin-secreting cells. *Br. J. Pharmacol.*, **103**,
2021–2029.

Lilja, J.J. *et al.* (1998) Grapefruit juice—simvastatin interaction: Effect on serum
concentrations of simvastatin, simvastatin acid, and HMG-CoA reductase inhibitors*.
Clin. Pharmacol. Ther., **64**, 477–483.

Lynch, J.J. *et al.* (2017) Potential functional and pathological side effects related to off-

target pharmacological activity. *J. Pharmacol. Toxicol. Methods*, **87**, 108–126.

Maechler, P. *et al.* (2010) Role of mitochondria in beta-cell function and dysfunction. *Adv. Exp. Med. Biol.*, **654**, 193–216.

McHugh, D. and Beech, D.J. (1996) Modulation of Ca2+ channel activity by ATP metabolism and internal Mg2+ in guinea-pig basilar artery smooth muscle cells. *J. Physiol.*, **492**, 359–376.

Nadanaciva, S. *et al.* (2007) Target identification of drug induced mitochondrial toxicity using immunocapture based OXPHOS activity assays. *Toxicol. Vitr.*, **21**, 902–911.

Narang, D. *et al.* (2013) Triton X-100 inhibits L-type voltage-operated calcium channels. *Can. J. Physiol. Pharmacol.*, **91**, 316–324.

O'Rourke, B. *et al.* (1992) Phosphorylation-independent modulation of L-type calcium channels by magnesium-nucleotide complexes. *Science*, **257**, 245–8.

Ohta, M. *et al.* (1990) Oxygen and Temperature Dependence of Stimulated in Isolated Rat Islets of Langerhans " Insulin Secretion. **265**, 17525–17533.

Ohya, Y. and Sperelakis, N. (1989) ATP regulation of the slow calcium channels in vascular smooth muscle cells of guinea-pig mesenteric artery. *Circ.Res.*, **64**, 145–154.

Real, J. *et al.* (2018) Lipophilicity predicts the ability of nonsulphonylurea drugs to block pancreatic beta-cell K $_{ATP}$ channels and stimulate insulin secretion; statins as a test case. *Endocrinol. Diabetes Metab.*, **1**, e00017.

Rorsman, P. *et al.* (1992) Cytoplasmic calcium transients due to single action potentials and votlage-clamp depolarizations in mouse pancreatic B-cells. **1**, 2877–2884.

Sattar, N. *et al.* (2010) Statins and risk of incident diabetes: a collaborative meta-analysis of randomised statin trials. *Lancet*, **375**, 735–742.

Schulla, V. *et al.* (2003) Impaired insulin secretion and glucose tolerance in beta cell-selective Ca(v)1.2 Ca2+ channel null mice. *EMBO J.*, **22**, 3844–54.

Shi, J.-H. *et al.* (2017) Characterization of interactions of simvastatin, pravastatin,

fluvastatin, and pitavastatin with bovine serum albumin: multiple spectroscopic and molecular docking. *J. Biomol. Struct. Dyn.*, **35**, 1529–1546.

Sirvent, P., Bordenave, S., *et al.* (2005) Simvastatin induces impairment in skeletal muscle while heart is protected. *Biochem. Biophys. Res. Commun.*, **338**, 1426–1434.

Sirvent, P., Mercier, J., *et al.* (2005) Simvastatin triggers mitochondria-induced Ca2+ signaling alteration in skeletal muscle. *Biochem. Biophys. Res. Commun.*, **329**, 1067–1075.

Smith, P.A. *et al.* (1999) Direct effects of tolbutamide on mitochondrial function, intracellular Ca2+ and exocytosis in pancreatic β-cells. *Pflugers Arch. Eur. J. Physiol.*, **437**, 577–588.

Smith, P.A. *et al.* (1989) Modulation of dihydropyridine-sensitive Ca2+ channels by glucose metabolism in mouse pancreatic β-cells. *Nature*, **342**, 550–553.

Smith, P.A. (2009) N-Type Ca $^{2+}$ -Channels in Murine Pancreatic ?-Cells Are Inhibited by an Exclusive Coupling with Somatostatin Receptor Subtype 1. *Endocrinology*, **150**, 741–748.

Smith, P.A. *et al.* (1993) Permeation and gating properties of the L-type calcium channel in mouse pancreatic beta cells. *J. Gen. Physiol.*, **101**, 767–797.

Smith, P.A. *et al.* (2001) Somatostatin activates two types of inwardly rectifying K $^+$ channels in MIN-6 cells. *J. Physiol.*, **532**, 127–142.

Urbano, F. *et al.* (2017) Atorvastatin but not pravastatin impairs mitochondrial function in human pancreatic islets and rat β-cells. Direct effect of oxidative stress. *Sci. Rep.*, **7**, 1–17.

Wallace, K.B. (2008) Mitochondrial off targets of drug therapy. *Trends Pharmacol. Sci.*, **29**, 361–366.

Wang, E.J. *et al.* (2001) HMG-CoA reductase inhibitors (statins) characterized as direct inhibitors of P-glycoprotein. *Pharm. Res.*, **18**, 800–806.

Yada, T. *et al.* (1999) Inhibition by simvastatin, but not pravastatin, of glucose-induced cytosolic Ca2+ signalling and insulin secretion due to blockade of L-type Ca2+ channels in rat islet beta-cells. *Br. J. Pharmacol.*, **126**, 1205–1213.

Zhou, J. *et al.* (2014) Effects of simvastatin on glucose metabolism in mouse MIN6 cells. *J. Diabetes Res.*, **2014**, 376570.
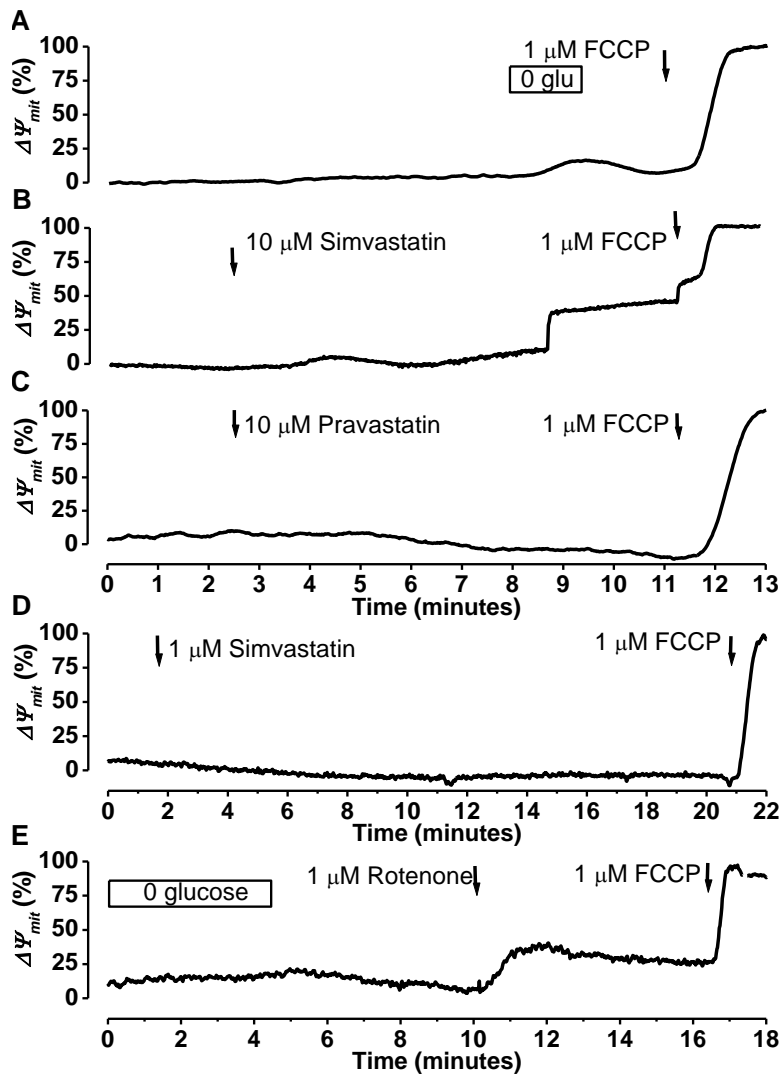
Figures and legends

Fig. 1. Simvastatin depolarizes the inner mitochondrial membrane potential, $\Delta\psi_{mit}$. Representative traces of Rh123 fluorescence for primary mouse β-cells recorded in response to conditions indicated. Arrows show the points where drugs were perifused. All in the presence of 5 mM glucose, unless otherwise indicated. Each record is the average of

several cells viewed within a given field normalised as a percentage of their response to 1 µM FCCP. A) Effect of glucose removal. B) Effect of 10 µM simvastatin, a lipophilic statin. C) Effect of 10 µM pravastatin, a lipophobic statin. D) Effect of 1 µM simvastatin. E) Effect of glucose removal and 1 µM rotenone.
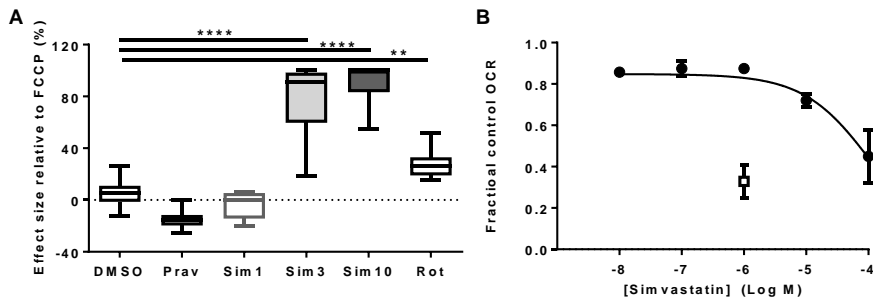
Fig. 2. Simvastatin inhibits mitochondrial function in murine beta-cells. A) Effect of 0.1%

vol/vol DMSO (n = 10), 10 µM pravastatin (Prav; n = 10), 1 µM simvastatin (Sim1; n = 5), 3

µM simvastatin (Sim3, n = 14), 10 µM simvastatin (Sim10; n = 16) and 1 µM rotenone (Rot,

n = 71) on Rh123 fluorescence as a percentage of that produced by 1 µM FCCP in primary

mouse pancreatic beta-cells. Data are from 7 preparations and are shown as the median,

inter-quartile and 10-90% values. Statistical comparison by Kruskal Wallis with Dunn's

multiple comparison test. B) Simvastatin concentration-effect relationship for the block of

glucose-stimulated oxygen consumption (OCR) in MIN6 beta-cells. Data, closed squares,

are shown as mean ± S.E.M (n= 5-9). Solid line is drawn to equation 1 with values given in

the text. The open square is the mean± S.E.M effect produced by 1 µM rotenone on glucose-
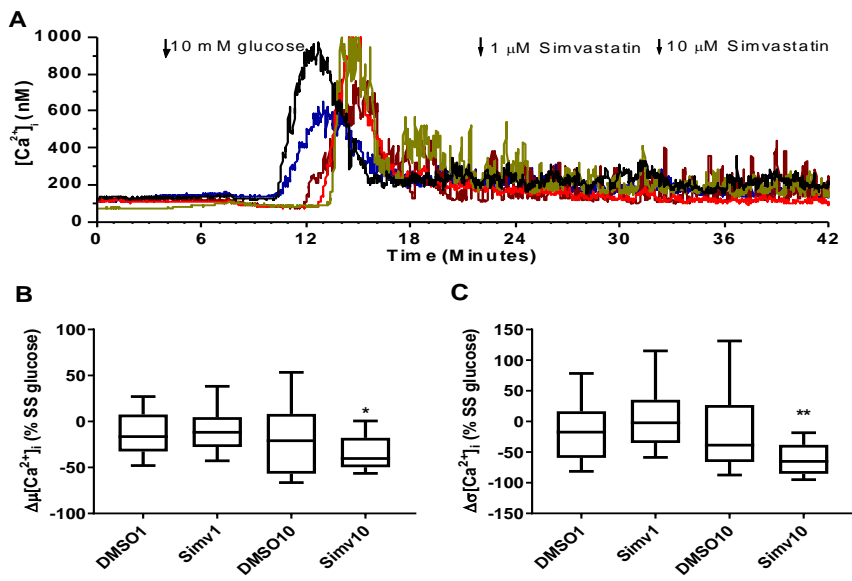
stimulated OCR (n= 11).

Fig. 3. Glucose elicits calcium influx, which is inhibited by simvastatin. A) Representative intracellular calcium, $[Ca^{2+}]_i$, traces for five MIN6 beta-cells clusters all recorded in the same field in response to the conditions indicated. Additions are perifused from the indicative arrows. B-C) Effect of 1 μM simvastatin (Simv1; n = 42) and its control 0.1% vol/vol DMSO (DMSO1, n = 42), and 10 μM simvastatin (Simv10; n = 34) and its control, 1% vol/vol DMSO (DMSO10, n = 44), on mean $[Ca^{2+}]_i$ (B) and its standard deviation (C) as a percentage of that measured in 10 mM glucose in the absence of drug or its vehicle. In all cases statistical tests are between simvastatin and its relevant DMSO control either Students t-test or Mann-Whitney test. Data are from 9 preparations and are shown as the median, inter-quartile and 10-90% values.
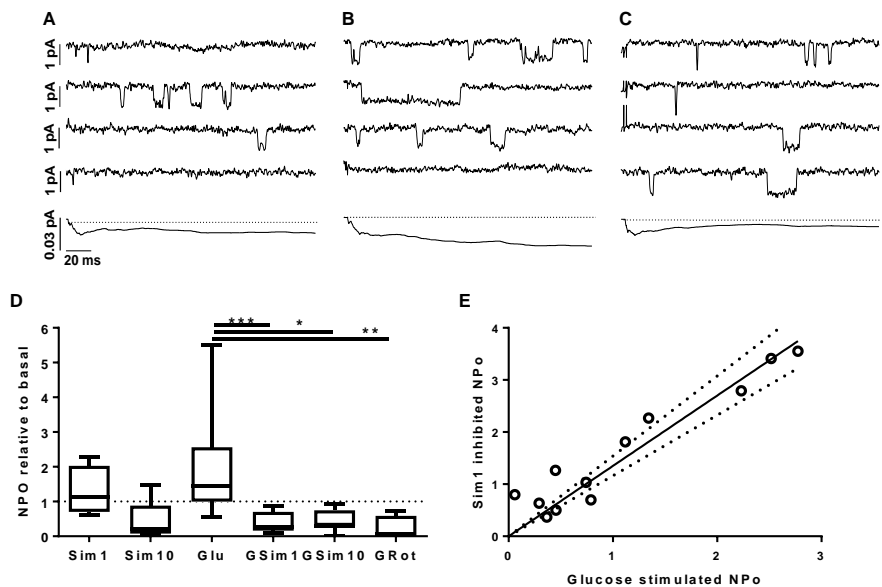
Figure 4. Simvastatin reverses the metabolic stimulation of L-type calcium channel activity. A-C) Single Ca^{2+} channel activity recorded from the same cell-attached patched on a MIN6 beta-cell. The pipette contained 10 mM Ba^{2+} and 0.1 µM BAY K 8644 to enhance resolution of single-channel currents. Currents were elicited by a step to -40 mV from a holding potential of -90 mV. Data filtered at 500 Hz. In each case the top four traces are consecutive records: A) Control conditions, B) after 5 minutes in 10 mM glucose, and then C) after 5 minutes in 10 mM glucose and 1 µM simvastatin. Lowest trace in each panel is the ensemble average of 100 traces. Note the increase in channel activity seen with glucose (B) relative to control (A), and how this was increase was reversed by simvastatin (C) back to control values (A). D) Changes in channel activity (NPo) relative to respective basal for the conditions indicated: 1 µM simvastatin on basal (Sim1; n = 5), 10 µM simvastatin on basal (Sim10; n = 6), 10 mM glucose (Glu; n = 14), 10 mM glucose + 1 µM simvastatin (GSim1; n

=14), 10 mM glucose + 10 µM simvastatin (GSim10; n = 7), 10 mM glucose + 1 µM Rotenone (GRot; n = 4). The effects of simvastatin and rotenone in the presence of glucose were statistically indistinguishable from each other (Kruskal Wallis Dunn's multiple comparison test) E) Relationship between inhibition of channel activity produced by 1 µM simvastatin in the presence of 10 mM glucose (Sim1) and the degree of stimulation produced by the sugar. Solid line is a fit to the data by linear regression with a slope of 1.35 ± 0.09; dotted lines are the 95% confidence intervals of the fit
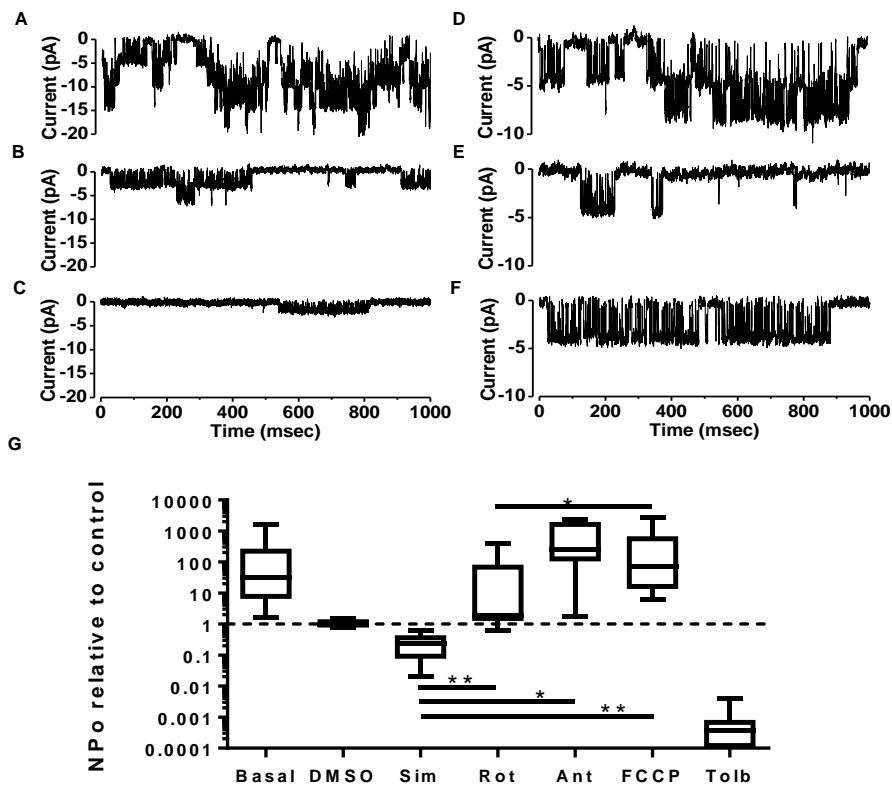
Figure 5. Effects of glucose and mitochondrial toxins on K_{ATP} channel. A-C) K_{ATP} channel activity recorded from the same cell-attached patched on a MIN6 beta-cell: A) Control conditions, B) after 5 minutes in 10 mM glucose, and then C) after 5 minutes in 10 mM glucose and 10 µM simvastatin. Note further block in activity with simvastatin. D-F) K_{ATP} channel activity recorded from a different cell-attached patched: D) Control conditions, E) after 5 minutes in 10 mM glucose, and then F) after 5 minutes in 10 mM glucose and 1 µM rotenone. Rotenone clearly activates the KATP channel in F) whereas in C) simvastatin leads to a further block. G) Changes in channel activity (NPo) relative to glucose for the conditions indicated except Tolbutamide which is relative to FCCP: Absence of glucose (Basa; n = 58), DMSO (DMSO; n = 4), 10 µM simvastatin (Sim; n = 6), 1 µM Rotenone (Rot;

n = 10) 1 µM Antimycin (Ant; n = 5), 100 nM FCCP (FCCP; n =25), 200 µM Tolbutamide (Tolb; n = 9). Statistical significance for the Sim, Rot, Ant and FCCP is with Kruskal -Wallis followed by an all pairwise post hoc test (Dwass-Steel-Chrichlow-Fligner). The effects of rotenone and antimycin in the presence of glucose were statistically indistinguishable from each other.